

CFD and Frictional Torque Analysis of Hydrodynamic Journal Bearing

Abhinav Maurya

Department of Mechanical Engineering
Delhi Technological University
New Delhi, India

Abhay Kumar

Department of Mechanical Engineering
Delhi Technological University
New Delhi, India

Aman Dev Punia

Department of Mechanical Engineering
Delhi Technological University
New Delhi

Abstract— This paper aims at CFD and frictional torque analysis of hydrodynamic journal bearing. Numerous experiments were performed on bronze bearing and two journals of different materials, mild steel and bronze for the frictional torque analysis using SAE10W40 lubricating oil on specially designed test rig. Graphs for frictional torque and coefficient of friction were plotted from results of experimental data and theoretical calculation. Results of both journals were compared for frictional torque and coefficient of friction was calculated experimentally and theoretically (using the Petroff's equation). It was observed that frictional torque increases as the shaft speed increase and becomes almost constant as the shaft approaches extreme speed.

Keywords — *Hydrodynamic Journal Bearing, Frictional Torque Analysis, Stribeck Curve, Reynold's Equation*

I. INTRODUCTION

Bearing, especially hydrodynamic bearings are used to support rotating shaft in numerous industries. Journal bearing generally, operates with hydrodynamic lubrication. It has a shaft or journal rotating in a bearing. In the bearing, the shaft rotates with a layer of lubricant separating the two parts [Note: journal is the part of shaft lying inside the bearing]. It is used when the load is light and the motion is continuous. Since the journal bearing has no rolling element as in other bearings, it is also known as radial load sliding contact bearing.

Hydrodynamic journal bearing (fig. 1) is a very simple yet critical component as there are numerous parameters involved in its proper working. Journal bearing works by creating a pressure difference by moving fluid from converging to diverging by wedging action of fluid due to moving body parts because of which hydrodynamic journal bearing surface velocity and gap generation varies. Friction in fluid film causes frictional force and wear which reduces performance efficiency and increases maintenance cost. In hydrodynamic journal bearing, there is metal-to-metal contact during start-up. However, during running condition, there is fluid film between the two moving surfaces resulting less power loss and increased efficiency.

Failure in the Journal Bearings occurs due to improper lubrication as it will cause more wear rate and thermal expansion. Lubricant keeps the moving parts' surface away

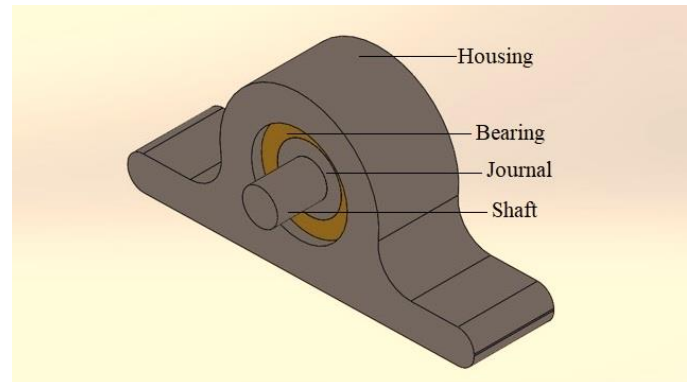


Fig. 1: Journal Bearing

from each other, acts as cooling agent and a medium to transfer additives to the machining area. Lubrication in the journal bearings is usually done by grooving that distributes and supplies the lubricant (placement of grooves is away from the load zone). Load, surface roughness, viscosity, speed, and clearances determine the correct oil film thickness for the specific application. It is often used in industrial machines that require high horsepower and high loads like turbines and pumps.

A. Basic Concept of Hydrodynamic Journal Bearing

The basic concept in hydrodynamic journal bearing is the lubricant action and its flow in between journal and the bearing, i.e. how the shaft is lifted by the lubricant to avoid metal-to-metal contact (see fig. 2). The lifting of the shaft is due to the wedging action (also called dynamic action or convergent action).

Steps in wedge development (Bearing speed is denoted by N):

- i. $N_1 = 0$ rpm, i.e. idle condition, the shaft rests on the bearing surface with normal reaction equal to the weight of the shaft.
- ii. $N_2 > N_1$, i.e. the working condition, even though the shaft has started rotating, the speed is very low. Thus, there is a constant contact between the bearing and the journal surfaces. At this speed, the pressure is maximum at the point of contact.
- iii. $N_3 > N_1$, i.e. at high speed (increasing rate), the shaft starts lifting off. As the shaft speed increases, due to the friction between the shaft and the lubricant, the lubricant enters under

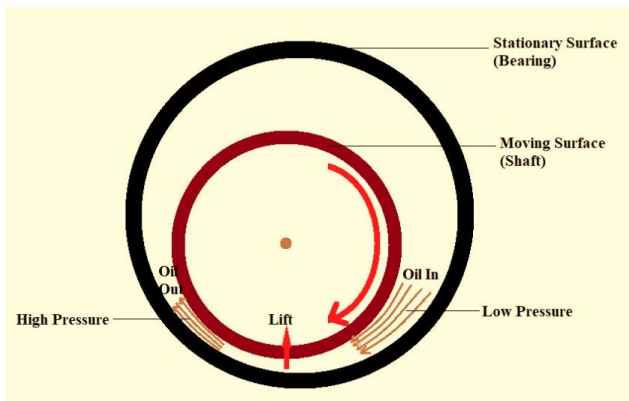


Fig. 2: Basic Development of an Oil Wedge

the shaft through converging action. Thus, lifting the shaft and the maximum pressure is at the location of minimum film thickness.

iv. $N_4 \gg N_1$ i.e. at high speed (constant or stable speed), the shaft is stable and the lubricant film thickness between the bearing and the journal in this situation is termed as minimum film thickness.

B. Frictional Torque

When the shaft is in stationary condition (absence of friction), the reaction offered by bearing is inline with a line of action of the load acting from the journal. When the shaft is in motion (presence of friction), the resultant R is deviated by distance x from the line of action of the load acting from the journal. A circle is drawn from the center of the shaft by taking radius x is known as friction circle.

Frictional Torque is given by,

$$T_f = \mu W r$$

where,

μ = Coefficient of friction

W = Load acting on bearing (N)

r = radius of bearing

The coefficient of friction, μ , can also be calculated using Petroff's Equation.

$$\text{Petroff's Equation: } \mu = 2\pi^2 \left(\frac{Zn}{P}\right) \left(\frac{D}{C}\right) + K$$

where,

$\frac{Zn}{P}$ = Bearing Characteristics Number

Z = Lubricant Viscosity (Pa-s)

n = Rotation per second

P = Pressure (Pa)

D = Bearing Diameter (mm)

C = Diametrical Clearance (mm)

K = Leakage Factor

$K = 0.002$ when $\frac{L}{D} < 0.75$

$K = 0.003$ when $\frac{L}{D} \geq 0.75$

C. Stribeck Curve

Stribeck curve (see fig.3) is a curve plotted between the coefficient of friction against the bearing parameter (ZN/P),

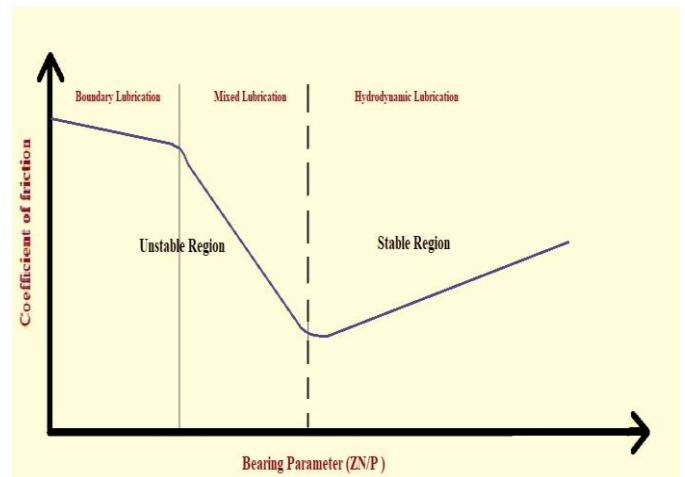


Fig. 3: Stribeck Curve

lubricant viscosity, N is rotating speed per second and P is bearing pressure. ZN/P is also known as bearing characteristics number (BCN).

- **Unstable Region:** Boundary lubrication and mixed lubrication regime lie in this region. In the boundary lubrication, there is a constant metal-to-metal contact hence the coefficient of friction is high. However, as we proceed towards the mixed lubrication, the coefficient of friction starts decreasing as the film thickness increases. In addition, due to the heat generated, the lubricant viscosity starts decreasing which reduces the effect of wedging action. Combining all the factors it can be noticed that as the BCN decreases, viscosity decreases and hence the coefficient of friction increases.

- **Stable Region:** Hydrodynamic lubrication regime lies in this region. As the journal speed increases, BCN increases and in addition to that heat generation also increases. In this case, amount of heat generation dominates, thus causing an increase in temperature of lubricant. Therefore, decreasing the lubricant viscosity and hence increasing the coefficient of friction. The point where the coefficient of friction is minimum is called bearing modulus.

In the unstable region, the power loss is dependent on the load applied. On the other hand, in the stable region, the power loss is dependent on viscosity instead of load applied.

D. Reynold's Equation

Reynold's equation is generally used in modelling of the hydrodynamic lubrication regime and is used to aid calculations. Pressure distribution in the lubricant can be expressed as a function of journal speed, bearing geometry, oil clearance and lubricant viscosity using Reynolds equation. There are certain assumptions made in hydrodynamic models:

- Negligible body forces
- Constant pressure throughout the film thickness
- No slip at the boundaries
- The lubricant is a Newtonian fluid (not true for polymeric oils)
- Flow is laminar (not true in large bearings)

- Fluid inertia is negligible
- Fluid density is constant (valid for liquid lubrication, not gas lubrication)
- Viscosity is constant throughout the film (not exactly true but it simplifies the problem)

$$\text{Reynold's equation: } \frac{\partial}{\partial x} \left(\frac{h^3}{\mu} \frac{\partial p}{\partial x} \right) + \frac{\partial}{\partial z} \left(\frac{h^3}{\mu} \frac{\partial p}{\partial z} \right) = 6U \frac{\partial h}{\partial x}$$

where:

h – local oil film thickness,
 η – dynamic viscosity of the oil,
 p – local oil film pressure,
 U – linear velocity of the journal,
 x - circumferential direction.
 z - longitudinal direction.

Close form solution of Reynolds equation can't be obtained therefore finite element method is used to solve it. Two analytical solutions of Reynolds equation exist only for above-mentioned assumptions. The two solutions are Sommerfeld and Ocvirk solutions, are applicable only in the region of positive pressure

- Sommerfeld Solution:

$$P = \frac{\eta Ur}{c_r^2} \left(\frac{6\epsilon(2 + \epsilon \cos\theta) \sin\theta}{(2 + \epsilon^2)(1 + \epsilon \cos\theta)^2} \right) + P_o$$

The equation is solved with the assumption that there is no lubricant flow in the axial direction (infinitely long bearing assumption).

- Ocvirk Solution: Ocvirk solution for infinitely short bearing assumption neglects circumferential pressure gradients (first term of Reynolds equation)

$$P = \frac{\eta Ur}{c_r^2} \left(\frac{B^2}{4} - z^2 \right) \left(\frac{3\epsilon \sin\theta}{(1 + \epsilon \cos\theta)^3} \right) + P_o$$

$$P = \frac{P_{cv}}{D^2 S_o} (B^2 - 4z^2) \left(\frac{3\epsilon \sin\theta}{(1 + \epsilon \cos\theta)^3} \right) + P_o$$

where,

C_r : radial clearance
 ϵ : eccentricity ratio
 B: bearing length,
 P_o : cavitation pressure,
 S_o : Sommerfeld number.

The Sommerfeld number remains constant for a given bearing and is used to correlate working condition of the different machine working with the same bearing. Sommerfeld number is analogous to the human fingerprint, i.e, every bearing has its own unique Sommerfeld number. It is given by

$$\text{Sommerfeld Number: } S_o = \frac{ZN}{P} \left(\frac{D}{C} \right)^2$$

II. CFD ANALYSIS

In this research work, the pressure distribution in the lubricating fluid regime was solved in which the inlet of fluid was provided through the mid-section and the outlet of the fluid was taken at the end walls of the bearing at both sides. Further, the result obtained was used to solve for the deformation, stresses, strain etc. The CFD analysis was applied to mathematically check whether the pressure distribution in the fluid film was same as experimental. Different simplifying assumptions, based on experimental observations were used to solve the characteristics of bearing. The assumption was made that the viscosity of fluid film remains same and does not vary with the temperature. The energy equation was applied with the assumption that the regime of flow to be laminar. The bearing load was applied along with the effect of fluid pressure contour on the bearing was applied to calculate the stresses, strain, strain energy, deformation of the bearing. The solution was done with the use of CFD and ANSYS Fluent software.

A. Geometrical modelling and Meshing

The bearing material taken is Bronze (86% copper, 9.5% tin, 2.5% lead, and 2% zinc). However, the materials used for the journals were Bronze (86% copper, 9.5% tin, 2.5% lead, and 2% zinc) and Mild steel (0.05%-0.25% carbon and up to 0.4% manganese, rest Iron). The design of journal bearing was made with the help of ANSYS 15.0 (see fig. 4), the dimensions of which are shown in table 1.

For the fluent analysis, the journal and bearing were suppressed and the fluid film between them having a thickness of 27 microns was considered. The mesh was generated over the fluid film (fig. 5). The named selection was created where the inlet was provided in the mid-section of the fluid film and the outlet was marked at the end of the plane surface.

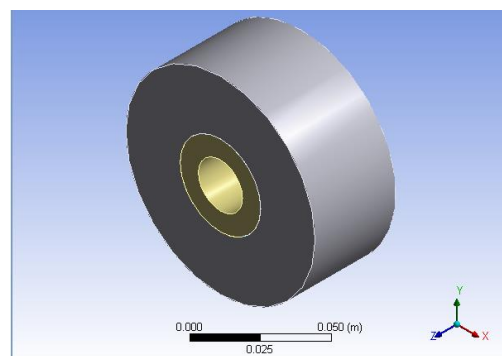


Fig 4: 3D Model of the journal bearing in ANSYS

TABLE 1: DIMENSIONS OF JOURNAL BEARING MODEL USED IN ANSYS

S.No	Part Detail	Range
1.	Shaft Diameter	22+0.005mm
2.	Journal Outer Diameter	40-0.005/0.006mm
3.	Journal Inner Diameter	22.035mm
4.	Bearing Inner Diameter	40+0.050/0.06mm
5.	Bearing width	40.04mm
6.	Radial Clearance	0.027mm
7.	L/D ratio	1

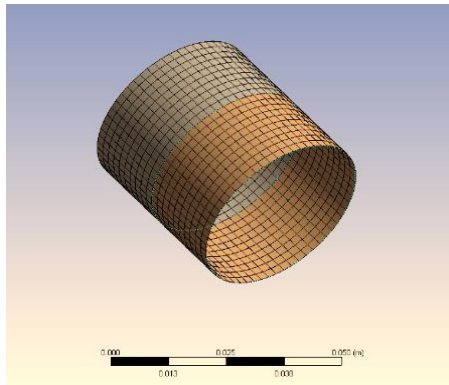


Fig 5: Meshing of fluid film showing named selection in ANSYS 15.0

B. Solution

For solution, the laminar flow was selected and the energy equation was turned on. The material of the fluid was then input as given below. The properties of the lubricant used (SAE10W40) was entered as the data mentioned in Table 2. After this, the boundary conditions were inserted in which the velocity inlet criteria was followed. The inlet velocity was taken as 10m/s and the inlet pressure was taken as 101325 pascals. The temperature of the fluid inlet was taken to be around 320K. After running iterations and solving the pressure distribution on the journal bearing was found as pressure contour.

TABLE 2: LUBRICANT PROPERTIES

S.No.	Parameter	Value
1.	Journal Radius	40 mm
2.	Radial Clearance, C	27µm
3.	Lubricant Viscosity, µ	0.079 kg/ms
4.	Lubricant Density	845 kg/m ³
5.	Lubricant specific heat, Cp	1901.07J/kg°C
6.	Lubricant thermal conductivity	0.1242

C. Analysis of Journal Bearing

In the static analysis, the mesh was generated around the bearing (fig. 6), then the load was imported from the previous contour at the inner surface of the cylinder. The bearing load was also inserted in the component form (fig. 7). The solution was done and various results for the equivalent stress, strain, deformation and strain energy was calculated. The bearing material properties considered are shown in table 3.

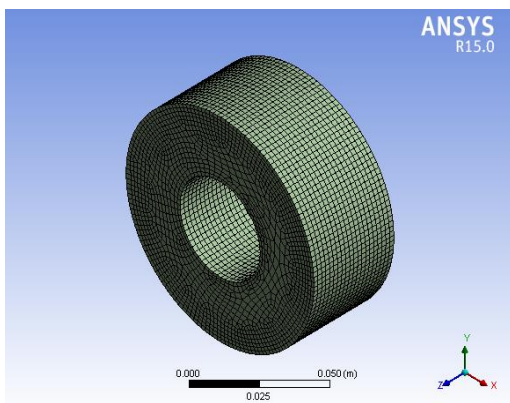


Fig 6: Mesh generation on bearing

TABLE 3: BEARING MATERIAL PROPERTIES

S.No.	Property	Value
1	Density	8719 kg/m ³
2	Young's Modulus	103 GPa
3	Poisson' Ratio	0.34
4	Bulk Modulus	116 GPa
5	Shear Modulus	40 GPa

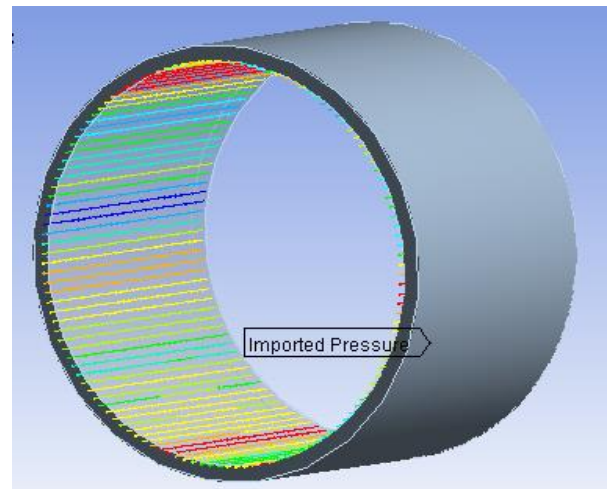


Fig 7: Pressure imported on bearing

III. MODELLING BASED ON EXPERIMENTAL TEST RIG

A. Main Designing Frame

The Journal Bearing Rig TR-660 (fig. 8-10) was used to demonstrate the frictional torque and pressure distribution inside bearing. Table 4 gives the mechanical specifications of the test rig. The journal was mounted horizontally on a shaft supported on a self-aligning bearing and a motor with timer bolt rotates the shaft. A leaded bronze, flawless bearing freely slides over the journal and as it rotates radial load was applied on bearing by pulling it upwards against journal by a loading lever. Ten sensors were fixed on the circumference of bearing with their terminal ends ending in a junction box. The journal was driven by a belt and two-step pulley arrangement and speed required was set on software. Radial load and journal speed were varied to suit the test conditions. The testing oil used for the experiment was SAE 10W40.

A ground shaft was supported on two self-aligned bearings on either end of the oil sump. The oil sump was wide enough to house the bearing with all sensors with the connector inside it. To attain a low speed of 40rpm and max speed of 8000rpm, two-step pulleys having a ratio of 1:4 and 4:1 ratio were fixed on shaft and motor ends. A motor having a base speed of 1435rpm was mounted over base plate drives the shaft.

The loading lever having load ratio 1:5 was fixed on a frame, the frame height was kept sufficiently high to minimize the reduction of radial load due to the inclination of loading lever when max weight was placed. The loading lever was pivoted to a vertical frame, smaller end of the lever was connected to bearing top through a wire rope, on either end of wire spherical eye bolt was fixed to give free angular movement.



Fig. 8: TR660 Journal Bearing Test Rig

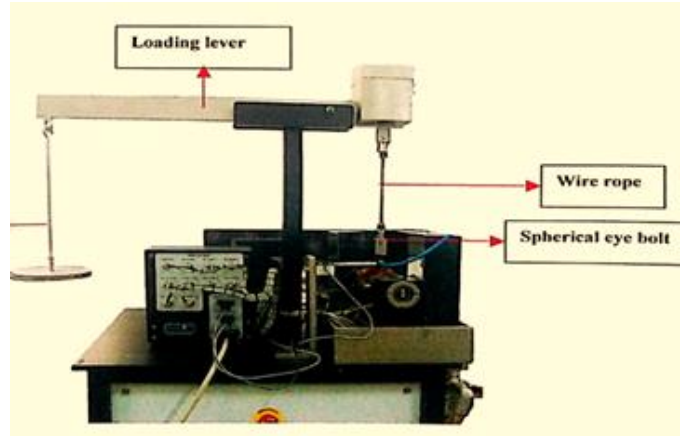


Fig 9: Loading System

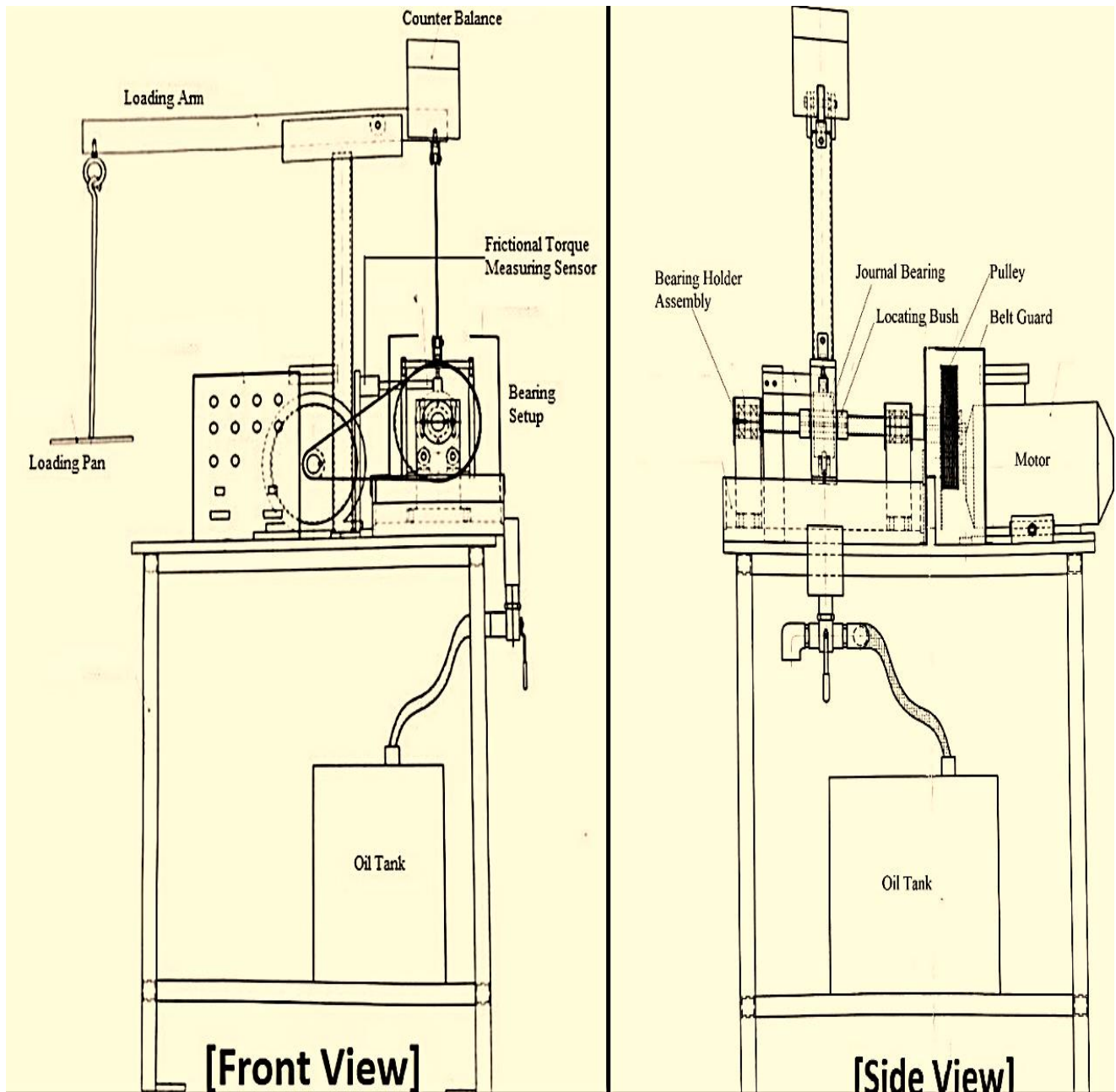


Fig. 10: Front view and side view of the journal bearing test rig

TABLE 4: MECHANICAL SPECIFICATIONS OF THE TEST RIG

S.No	Part Detail	Range
1.	Shaft Diameter	22+0.005mm
2.	Journal Outer Diameter	40-0.005/0.006mm
3.	Journal Inner Diameter	22.035mm
4.	Bearing Inner Diameter	40+0.050/0.06mm
5.	Bearing Outer Diameter	95mm
6.	Bearing width	40.04mm
7.	Radial Clearance	0.027mm
8.	L/D ratio	1
9.	C/R Ratio	0.00135
10.	Max. Load	3000N
11.	Loading Ratio	1:5
12.	Frictional Torque Distance	51mm
13.	Spindle Speed (min.)	40 rpm
14.	Spindle speed (max.)	8000 rpm
15.	Lubrication Unit (Oil Pressure)	5-10 bar
16.	Lubrication Unit (Tank Capacity)	25 L
17.	Lubrication Unit (Size l*b*h)	370 x 290 x 300mm
18.	Lubrication Unit (make)	Cenlube System
19.	Oil Hole (external surface)	13mm
20.	Oil Hole (internal surface)	6mm

B. Measuring system – Frictional Torque Sensor

The measuring system measures frictional torque and records the data. Table 5 shows the specification of the frictional torque sensor. This system consists of computer, signal processing modules and measuring devices as its main components. A beam type load cell 30kg capacity was fixed on to the oil sump; the frictional arm touches the oil inlet researching from the bearing. During the journal rotation, the force exerted was transferred to the load cell that was measured and displayed on the computer screen. The torque distance was 51mm.

TABLE 5: SENSOR SPECIFICATIONS

Part Detail	Specification
1. Speed	
• Sensor	Output From Drive
• Range	40-8000rpm
• Least Count	1rpm
• Accuracy	(1±2% measured speed)rpm
2. Frictional Torque	
• Sensor	Beam Type load cell make: Sontronics, cap 30 kg
• Range	15Nm
• Least Count	0.01Nm
• Accuracy	(0.1±1% measured value) Nm

IV. EXPERIMENTAL ANALYSIS

A. Procedure

The experiment was conducted for two different materials for the journal, mild steel and bronze with the bearing made of

bronze. The following procedure was for the journal made of mild steel.

1. Selection of test bearing: The test bearing made of Bronze, with an inner diameter of 40.06mm was used. The bearing was a square bearing i.e. the l/d ratio of the bearing was one.

2. Selection of journal: Journal was selected according to the c/r ratio required. The journal selected has c/r =0.00135 and the outer diameter of the journal was 40.005mm.

3. Machine preparation for testing: Power input cable was connected to 220V, 50Hz, 3 phase supply. Then the machine was turned on by switching on the MCB on machine side panel, followed by switching on the lubrication motor.

4. Preparation of bearing for test:

- a. Split housing on either end of the self-aligned bearing was loosened and removed.
- b. A bush holder and the journal was inserted into the shaft and slide the other bush holder.
- c. The bearing was placed inside the oil sump at middle and the bracket was inserted over the bearing.
- d. Shaft with the journal was pushed through the test bearing and was provided with support on the bearing.
- e. Lock nuts on either side of the self-aligned bearing were tightened.
- f. Driven pulley was tightened onto the shaft, followed by loosening the motor position and aligning the driver pulley in line with driven pulley.
- g. The belt was passed over the pulleys and the nuts were tightened using four screws to lock the motor position.
- h. The weight of 1kg-wt was placed over the loading pan, followed by pushing the bracket upwards and moving the bearing inside the bracket.
- i. The bearing inside the bracket was positioned properly and the journal was pushed till it was inside the bearing.
- j. Finally, the journal was locked in place by clamping the bush holder.

5. Setting the computer for test:

- a. Winducom 2008 software was opened and was ran in continuous mode for operating software.
- b. The acquiring screen was opened by clicking ACQUIRE button.
- c. The file name was entered in the remarks column.
- d. Required journal speed was set by entering the value and the applied load was entered in load column.
- e. The START button was clicked followed by the INITIALISE button to bring pressure button to zero and ZERO button to bring the frictional torque to zero.

6. Testing:

- a. Lube unit was turned on and the oil was allowed to run for some time.

- b. It was ensured that the oil was flowing from either end of the bearing.
- c. 500rpm was selected from the speed range: 500rpm or 8000rpm, and the required speed (initially 50rpm) was entered in the respective window (the actual bearing speed was 37 times the entered speed)
- d. Clicked on RUN MOTOR to start shaft rotation.
- e. After the set speed was reached, dead weight was placed on loading pan.
- f. The frictional torque reading was noted for the given load after 10 seconds.
- g. Clicked on MOTOR STOP.
- h. The same process was repeated for various loads (10N, 20N, 30N, 40N 50N) and for various speeds (entered value were 50rpm, 60rpm, 70rpm, 80rpm, 90rpm).

Similarly, the experiment was conducted for the journal made of bronze by replacing the journal made of mild steel and the readings were noted.

B. Precautions taken during the testing

- a. To prevent the machine damage, the bearing temperature was not allowed to exceed 125°C.
- b. The lubricant was allowed to be cooled down to prevent viscosity changes.
- c. After five consecutive readings, the machine was turned off to allow the bearing and the lubricant to be cooled down.

V. RESULTS AND DISCUSSION

A. Results of CFD analysis

The pressure contour generated on the fluid film depicts that the pressure distribution varies greatly around the journal. The pressure was varying along the circumference of the oil film and the pressure being maximum on the lower side of the oil film, in this region the film was convergent. This can be related to the wedging action of the fluid film in which the pressure was maximum near the minimum film thickness region (see fig. 11). Similar results were also obtained for the stress using static analysis (fig. 12). This was validated with experimental as well as analytical results.

The various other results related to the deformation and stress in the bearing due to the film pressure and bearing load was also calculated using the computational fluid dynamics. The deformation in the bearing can be related to the pressure wave generated around the circumference of the bearing due to converging and diverging phenomena respectively in the direction of rotation. This result showed that net deformation was maximum at lower left part of the bearing when the rotation was clockwise during the startup (see fig. 13).

B. Results of Frictional torque

The frictional torque was calculated for the various load and rotation of the shaft. The shaft and journal were made of stainless steel, the bearing was made of bronze. On this setup

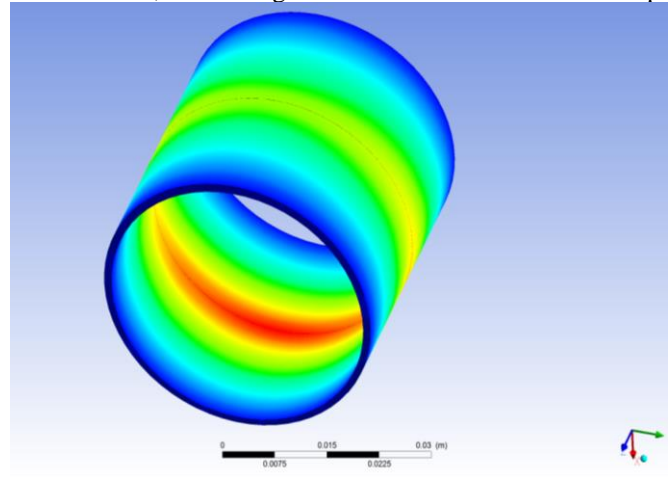


Fig 11: Pressure contour of the oil film using ANSYS Fluent

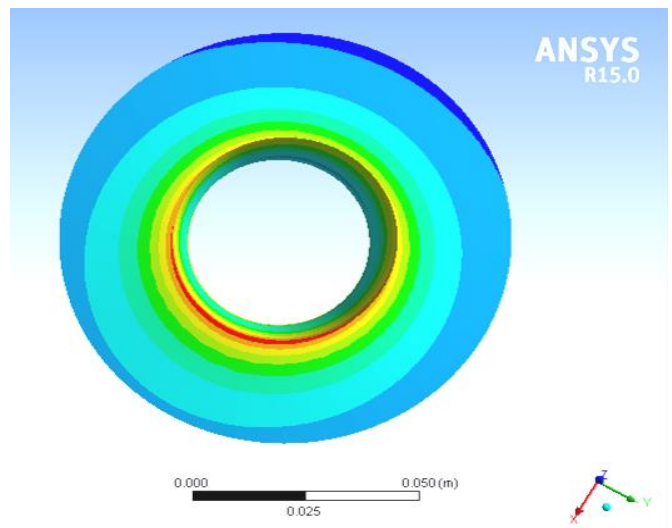


Fig 12: Stress in the bearing using ANSYS static analysis

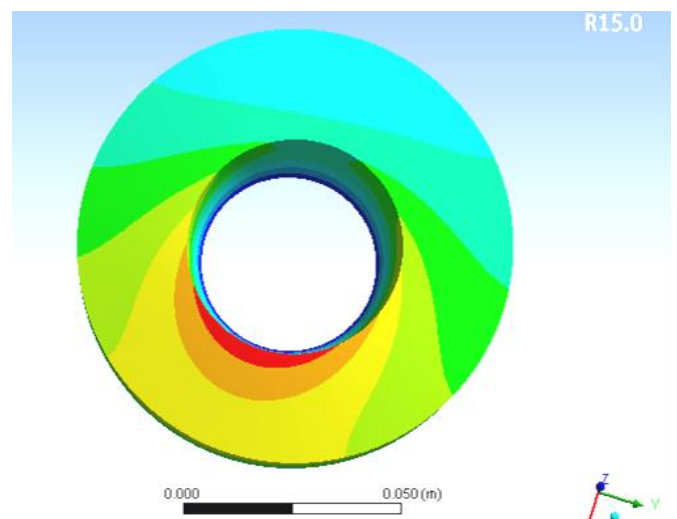


Fig 13: Total deformation in bearing using ANSYS structural analysis

the load was applied as 100N, 150N and 250N and the rotation speed were varied as 1850rpm, 2200rpm, 2600rpm, 3000rpm, 3350rpm. The load ratio provided was of 1:5 and the frictional torque distance was 51 mm.

The frictional torque was calculated for the various load and the graph was plotted against shaft speed (in rpm), where the frictional torque (in Nm) was plotted on the y-axis and shaft speed (in rpm) was plotted on the x-axis for various loads as earlier mentioned (see fig. 14). It was observed that the frictional torque increases with increase in shaft speed but become almost constant at high speeds.

C. Results of the Coefficient of friction

Variation of co-efficient of friction was plotted against shaft speed (in rpm), where the coefficient of friction was plotted on the y-axis and shaft speed was plotted on the x-axis for various loads. For the bearing load of 250N, the coefficient of friction was calculated using experimental data obtained through specifically designed test rig machine. In addition, for the same load of 250N, the theoretical value of the coefficient of friction was calculated using the Petroff's equation for various speeds of the shaft provided.

The results obtained were then plotted to show the variation of coefficient of friction with varying speed of shaft for experimental and theoretical results (see fig. 15).

The experimental and theoretical result shows that the coefficient of friction increases as the speed of rotation of shaft increases. It was observed from the experimental data that the coefficient of friction between the journal and the bearing was varied from 0.2 to 0.35 and the average calculated value was 0.301. However, from the theoretical data, it was observed that the value of the coefficient of friction was varying from 0.25-0.31 and the average calculated value was 0.283.

D. Effect of the Material of Journal on Frictional Torque

The effect of journal material on the frictional torque was calculated employing the two different materials, one was mild steel and another was bronze alloy. The result of frictional torque was obtained for both the material and graph was plotted to represent them graphically (see fig. 16). The load applied was 250N and the rotating speed of the shaft was varied from 1850 to 3350 rpm.

For two type of shaft material (steel and bronze) variation of frictional torque was plotted against shaft rpm in which frictional torque was on y-axis and shaft speed in rpm on the x-axis at 250N load. The graph plotted to depict that the frictional torque in a journal made of bronze was less than that of bronze for the same speed of the shaft.

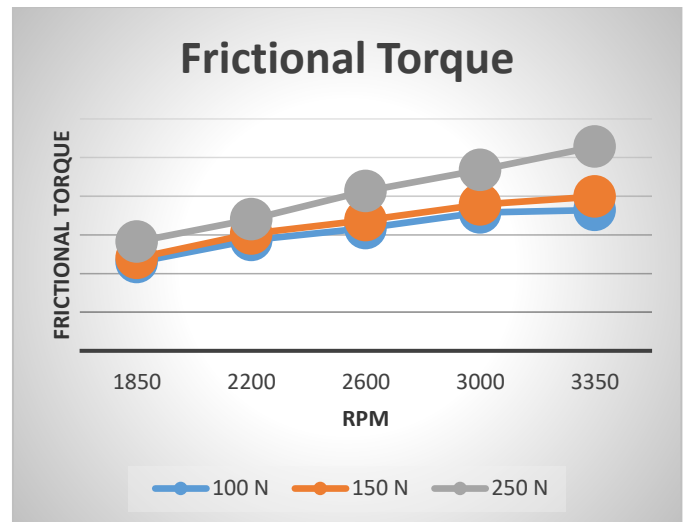


Fig 14: Variation of Frictional Torque with Speed for the various loads

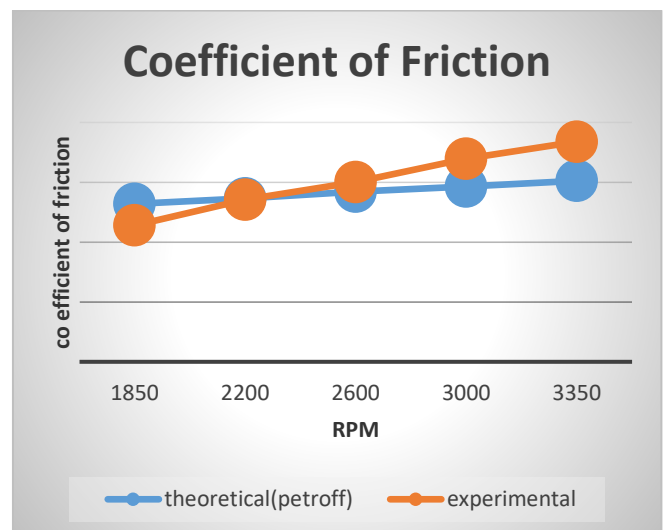


Fig 15: Graph representing the variation of coefficient of friction theoretically and experimentally with shaft speed at the applied load of 250N

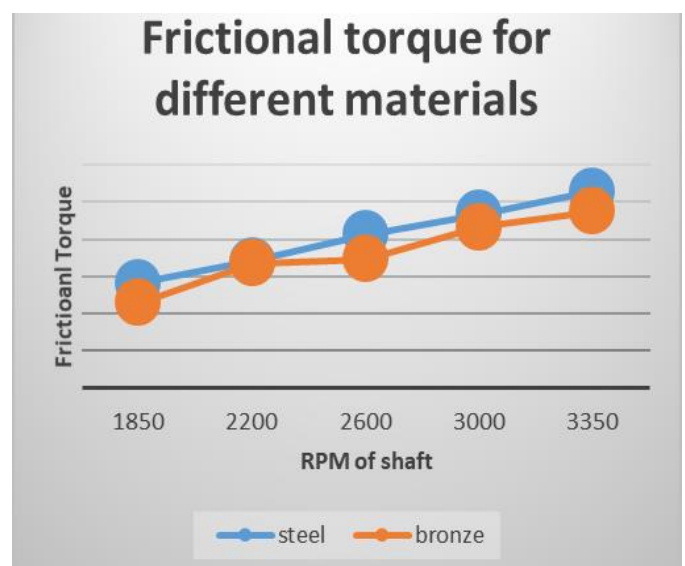


Fig 16: Variation of Frictional Torque with Speed for a load of 250N for the two journal materials (mild steel and bronze)

VI. CONCLUSION

a) The computational fluid dynamics of pressure distribution around the fluid film showed that the pressure variation along the circumference is varying greatly. The pressure being maximum near the minimum film thickness region. The result can be further used to design bearing in such a way that it could bear the stress generated in various region. The pressure contour generated could be related with the mathematical results obtained by solving the Reynold's equation. This CFD analysis can be further proved with the help of experimental results obtained by specially designed test rigs.

b) The frictional torque value obtained by the experimental results on the bearing showed that the torque increases with increasing load at the given spindle speed. the lubricating oil SAE 10-W40 was used and It showed that with increase in spindle speed at given load the frictional torque increases for low range speed. The graph generated also showed that the frictional torque becomes almost constant above 3000 RPM.

c) The coefficient of friction calculated experimentally and theoretically using Petroff's equations at 250 N load. The experimental value of coefficient of friction is about 0.301 and the theoretical value calculated using the various parameters is 0.273. The percentage error in the result is around 10.2%. This showed that experimental analysis can be related with the mathematical equations for hydrodynamic journal bearing.

d) The frictional torque was calculated for different materials of same dimensions. A steel journal and another bronze alloy journal was installed on the test rig to calculate the frictional torque having SAE 10-W40 as lubricating oil. The result showed that frictional torque in bronze is somewhat less than frictional torque in journal made of mild steel. This can be related with the fact that bronze has 2.5% lead in its composition. As lead is a self-lubricating metal it reduces the friction between the bearing and journal. Thus, bronze bearing can be used instead of mild steel as it experiences less friction, but it also experiences more wear than mild steel journal as it a soft metal. Lead is also injurious for health as it can result in pollution of ground and can cause hazards to human.

VII. FUTURE SCOPE

1. Pressure measurement can be done over the bearing surface using experimental analysis.
2. Different lubrication regimes can be studied to evaluate frictional torque.
3. Different lubricants can be studied to find the frictional torque between the bearing and the journal
4. The effect of temperature on viscosity can be studied to examine the dependence of frictional torque on viscosity
5. Different materials can be used for journal to further reduce the frictional torque.
6. Use of organic materials for the journal and the bearing for the study of frictional torque
7. Use of nanomaterials as solid lubricant to reduce the frictional torque

8. Experimental fluid film thickness can be measured at different locations on the periphery of the journal.

REFERENCES

- [1] Allaire, P.E., Kocur, J.A., and Nicholas, J.C., 'A pressure parameter method for the finite element solution of Reynolds equation', 39th ASLE annual meeting, Chicago, May 7-10, 1984.
- [2] B.C Majumdar, "Introduction to tribology of bearings," S. Chand 2008.
- [3] Bathe, K.J., "The Finite Element Method." Prentice-Hall, 1996.
- [4] Bearings and Their Lubrication by L. P. Alford, McGraw Hill, The American Machinist, 1911.
- [5] Chetan Mehra, Amar Singh Kokadiya, "Study of Pressure Profile in Hydrodynamic Lubrication Journal Bearing".
- [6] D. M. Nuruzzaman, M. K. Khalil, M. A. Chowdhury, M. L. Rahaman, "Study on Pressure Distribution and Load Capacity of a journal Bearing Using Finite Element Method and Analytical Method," International Journal of Mechanical & Mechatronics Engineering, vol. 10, p. 8 2010.
- [7] Dassault Systemes, SIMULIA Abaqus, 6.12 Theory Manual., 2012. p. 1173.
- [8] DIN 31652-1, "Plain bearings; hydrodynamic plain journal bearings designed for operation under steady-state conditions; design of circular cylindrical bearings," April 1, 1983.
- [9] DIN 31652-2, "Plain bearings; hydrodynamic plain journal bearings designed for operation under steady-state conditions; functions necessary when designing circular cylindrical bearings," February 1, 1983.
- [10] Dinesh Dhande1, Dr D W Pande2, Vikas Chatarkar, "Analysis of Hydrodynamic Journal Bearing Using Fluid Structure Interaction Approach" (IJETT) - Volume4 Issue8- August 2013
- [11] Dresel W., Mang T., Editors: Lubricants And Lubrication. 2nd Edition. Weinheim: Wi-Ley-Vch; 2007.
- [12] H. Allmaier, C. Priestner, C. Six, H. H. Priebsch, C. Forstner, and F. Novotny-Farkas, "Predicting friction reliably and accurately in journal bearings—A systematic validation of simulation results with experimental measurements," Tribology International, vol. 44, pp. 1151-1160, 2011.
- [13] H. Allmaier, C. Priestner, C. Six, H. H. Priebsch, C. Forstner, and F. Novotny-Farkas, "Predicting friction reliably and accurately in journal bearings – A systematic validation of simulation results with experimental measurements," Tribology International 44 (2011) 1151–1160, May 2011.
- [14] H. Allmaier, C. Priestner, F. M. Reich, H. H. Priebsch, C. Forstner and F. Novotny-Farkas, "Predicting friction reliably and accurately in journal bearings – The importance of extensive oil-models" Tribology International 48 (2012) 93–101 November 2011.
- [15] H. Allmaiera, D. E. Sandera and F. M. Reich, "Simulating Friction Power Losses In Automotive Journal Bearings" Procedia Engineering 68 (2013) 49 – 55.
- [16] Harish Hirani, "Fundamentals of Engineering Tribology," Cambridge Education Press, March 2016.
- [17] K. P. Gertzog, P. G. Nikolakopoulos, C. A. Papadopoulos, "CFD analysis of journal bearing hydrodynamic lubrication by Bingham lubricant", Tribology International 41 (2008) 1190–1204.
- [18] M. D. Hersey, Laws of lubrication of journal bearings. Trans. ASME. 37, 167-202 (1915).
- [19] M. D. Hersey, Theory of Lubrication (John Wiley & Sons, Inc., London and New York, 1936).
- [20] Machine Design, Part III by International Textbook Company, 1907.
- [21] Malcolm E. Leader, P.E. "Understanding Journal Bearings", Applied Mechanics Co., 2007.
- [22] R. R. Navthar and N. V. Halegowda, "Experimental Investigation of Oil Film Thickness for Hydrodynamic Journal Bearings," Applied Mechanics and Materials, vol. 110-116, pp. 2377-2382, 2011.

- [23] Raja Shekar Balupari, "validation of finite element program for journal bearings -static and dynamic properties" University of Kentucky Master's Theses, 2004.
- [24] Ravindra M. Mane and Sandeep Soni, "Analysis of hydrodynamic plain journal bearing" EJAET 2015, 2(2): 92-101.
- [25] S. K. Basu, S. N. Sengupta, B. B. Ahuja, "Fundamentals of Tribology," New Deldi: Prentice-Hall of India Private Limited, 2006.
- [26] S. Kasolang and R. S. Dwyer-Joyce, "Observations of Film Thickness Profile and Cavitation Around a Journal Bearing Circumference," Tribology Transactions, vol. 51, pp. 231-242, 2008.
- [27] Salmiah Kasolanga, Mohamad Ali Ahmada, Rob-Dwyer Joyceb, Che Faridah Mat Taib, "Preliminary study of Pressure Profile in Hydrodynamic Lubrication Journal Bearing," Procedia Engineering 41 (2012) 1743 – 1749.
- [28] V.B Bhandari, "Design of Machine Elements," Tata McGraw Hill, Nov 2003.
- [29] Verseteeng H. K. & Malalasekera W. _An Introduction to Computational Fluid Dynamics', Longman Scientific & Technical publication.
- [30] W Batchelor and G. W. Stachowiak, "Engineering Tribology - 4th Edition," Elsevier, 2014.
- [31] W. F. Hughes, F. Osterle, —Temperature Effects in Journal Bearing Lubrication, Tribology Transactions, 1: 1, 210-212, First published on: 01 January 1958 (iFirst).
- [32] Yousuf Mansoor and Paul Shayler, "The effect of oil feed pressure on the friction torque of plain bearings under light, steady loads," Tribology International 119, 316–328, 2018.